Published in final edited form as:
J Biomed Mater Res A. 2013 June ; 101(6): 1531–1538. doi:10.1002/jbm.a.34611.

Winner for Outstanding Research in the Ph.D. Category for the 2013 Society for Biomaterials Meeting and Exposition, April 10–13, 2013, Boston, Massachusetts:

Osteogenic differentiation of adipose-derived and marrow-derived mesenchymal stem cells in modular protein/ceramic microbeads

Rameshwar R. Rao, **Alexis W. Peterson**, and **Jan P. Stegemann**
Department of Biomedical Engineering, University of Michigan, Ann Arbor

Abstract

Modular tissue engineering applies biomaterials-based approaches to create discrete cell-seeded microenvironments, which can be further assembled into larger constructs for the repair of injured tissues. In the current study, we embedded human bone marrow-derived mesenchymal stem cells (MSC) and human adipose-derived stem cells (ASC) in collagen/fibrin (COL/FIB) and collagen/fibrin/hydroxyapatite (COL/ FIB/HA) microbeads, and evaluated their suitability for bone tissue engineering applications. Microbeads were fabricated using a water-in-oil emulsification process, resulting in an average microbead diameter of approximately 130 ± 25 μm. Microbeads supported both cell viability and cell spreading of MSC and ASC over 7 days in culture. The embedded cells also began to remodel and compact the microbead matrix as demonstrated by confocal reflectance microscopy imaging. After two weeks of culture in media containing osteogenic supplements, both MSC and ASC deposited calcium mineral in COL/ FIB microbeads, but not in COL/FIB/HA microbeads. There were no significant differences between MSC and ASC in any of the assays examined, suggesting that either cell type may be an appropriate cell source for orthopedic applications. This study has implications in the creation of defined microenvironments for bone repair, and in developing a modular approach for delivery of pre-differentiated cells.

Keywords

cell therapy; stem cells; collagen; fibrin; modular tissue engineering

INTRODUCTION

Improved therapies for the regeneration of bone are needed to achieve full repair of recalcitrant and large fractures. Through the combination of cells, materials, and signaling molecules, tissue engineering aims to create biomimetic tissue constructs to both regenerate and replace damaged tissue.[1] Numerous sources of stem and progenitor cells[2] have been used in bone tissue engineering applications including embryonic,[3] umbilical cord,[4] and

Correspondence to: J. P. Stegemann; jpsteg@umich.edu.

dental pulp.[5] However, bone marrow-derived mesenchymal stem cells (MSC) and adipose-derived stem cells (ASC)[6] are the most commonly studied cell types for orthopedic applications and both have demonstrated the ability to regenerate bone *in vivo*.[7,8] Further, both of these cell types has specific advantages in their use; MSC have been suggested to have immunomodulatory properties[9] and therefore can be used as an allogeneic source. ASC have the advantage that they are an easily obtained autologous cell source.[10] A number of recent studies have directly compared the osteogenic potential of these two cell types; however the results are context-dependent and more work is needed to determine the utility of these cells in specific applications.[11–15]

Natural biomaterials such as collagen (COL),[16–18] fibrin (FIB),[19,20] and chitosan[21,22] have been proposed as osteo-conductive materials for engineering and regenerating bone. Ceramics such as β-tricalcium phosphate,[18] calcium carbonate,[23] bioglass,[24] or coatings created by simulated body fluid (SBF)[25] have been combined with these materials to enhance the mechanical properties and osteoinductivity of the matrices. In particular, incorporation of hydroxyapatite (HA), the principal mineral component of native bone, has proven to be an effective strategy to provide stem cell-specific cues that aid in the formation of biomimetic composite structures for the engineering of bone.[15,26,27]

Modular tissue engineering has emerged as a scheme for applying a “bottom-up” approach to fabricate engineered tissues.[28] Cell-seeded, modular hydrogel microenvironments (“microbeads”) can be individually cultured, differentiated, and then later combined to create macroscopic tissue constructs with defined architecture. In bone tissue engineering, recent studies have used gelatin microcarriers to support osteogenic differentiation of human amniotic fluid MSC which were then combined to create bone tissue constructs.[29] Other studies have used alginate microbeads to differentiate human embryonic stem cells toward the osteo-blast lineage.[30] Previous work in our lab has used various natural biomaterials including chitosan, FIB, COL, and aga-rose to create cell-seeded microenvironments through a water-in-oil emulsion process.[31–33] Pure protein microbeads have been difficult to fabricate using this process because they are difficult to harvest and are fragile. To circumvent this issue, the COL matrix can be supplemented with aga-rose to generate composite microbeads for osteogenic differentiation of encapsulated MSC.[34] However, the inclusion of agarose, a polysaccharide not found in bone, limits the application of such microbeads in bone repair.

In this study, we generated pure protein microbeads by combining COL and FIB for bone repair applications. Particulate HA was also added to the microbeads to increase the density of microbead preparations, thereby facilitating harvesting during the production process. Our primary goal was to directly compare the osteogenic differentiation of MSC and ASC in COL/FIB and COL/FIB/HA microbeads. These modular cell-based hydrogel microenvironments could provide utility in generating natural biomaterial based approaches to bone regeneration.

MATERIALS AND METHODS

Collagen/fibrin microbead fabrication

Microbeads composed of 50/50 (mass ratio) COL/FIB were generated through a water-in-oil emulsion technique as shown in Figure 1. Bovine type I COL (MP Biomedicals, Solon, OH) was dissolved in 0.02*N* acetic acid at a concentration of 4.0 mg/mL and bovine fibrinogen (Sigma Aldrich, St. Louis, MO) was dissolved at 4.0 mg/mL clottable protein in serum-free Dulbecco's modified Eagle's medium (DMEM; Thermo Scientific, Logan, UT). COL (1.25 mg/mL) and FIB (1.25 mg/mL) were then added to a mixture containing 10% fetal bovine serum (FBS; Life Technologies, Grand Island, NY), 10% 5×-concentrated DMEM (starting concentration), 5% 0.1*N* NaOH, 2% bovine thrombin (1 UT/mL; Sigma), and 1 m*M* glyoxal (Sigma) at 4°C. The remaining volume for HA-containing microbeads, 2.5 mg/mL of HA in 1± DMEM, was sonicated for 1 h prior to incorporation to ensure homogenous distribution throughout the microbeads.[35] The HA was then added directly into the pre-gel mixture.

The pre-gel mixture was then quickly pipetted into a pre-cooled bath of 100 cSt polydimethylsiloxane (PDMS; Xia-meter, Dow Corning, Midland, MI) and stirred with a double-bladed impeller set at 700 RPM. After 5 min of mixing at 4°C, the temperature was then raised to 37°C to initiate co-polymerization and gelation of the COL and FIB. Microbe-ads were collected from the oil phase by centrifuging the mixture at 200*g* and washing three times for 10 min per wash with phosphate buffered saline (PBS; Life Technologies) containing Pluronic L101 (BASF, Florham Park, NJ) in order to separate the beads from the oil phase and remove excess oil.

Microbead imaging, size, and size distribution quantification

For light microscopy imaging, microbeads were stained with EZBlue Coomasie reagent overnight and imaged with an Olympus IX15 Microscope system (Olympus America, Center Valley, PA). Confocal reflectance microscopy using a laser scanning microscope (Olympus) was used to acquire images of the microbead architecture. Microbead diameter was analyzed using ImageJ software (National Institute of Health, Bethesda, MD) and size and size distribution of the microbe-ads were quantified.

Cell culture

Human marrow-derived MSC (Lonza Inc., Walkersville, MD) and human ASC (Lonza) were grown in Minimum Essential Medium Alpha (αMEM) supplemented with 10% MSC-Qualified FBS and 1% penicillin/streptomyocin (Life Technologies). MSC were used at passage 6 and ASC were used at passage 5, corresponding to two subculture periods after arrival. Cells were added directly into the pre-gel mix at a concentration of 1.0×10^6 cells/mL to promote even cell distribution throughout the beads. Microbeads were cultured statically in 15-mL centrifuge tubes (Corning Incorporated, Corning, NY) with 3 mL of media.

Cell viability studies

Cell viability was assessed using a vital stain kit (Live/ Dead®, Life Technologies). At days 1 and 7, cell-seeded microbeads were collected and washed three times in sterile PBS for 10

min/wash. Microbeads were then incubated in a solution containing 4.0 μm calcein-AM and 4.0 μm ethidium homodimer-1 in PBS at 37°C for 35 min. Microbeads were again washed three times in PBS, and then imaged using a laser scanning confocal microscope (Olympus). Percent viability was calculated by comparing the total green-stained cells (live) to the total red-stained cells (dead).

Osteogenic differentiation

For osteogenic studies, cell-seeded microbeads were cultured in either complete medium (growth) or osteogenic medium composed of complete medium supplemented with 10 m*M* β-glycerophosphate (Sigma), 50 μg/mL ascorbic acid 2-phosphate (Sigma), and 100 n*M* dexamethasone (Sigma) for 14 days. Microbead samples were collected at days 1, 3, 7, and 14 and flash-frozen in liquid N_2 and stored at −80°C. To analyze cell proliferation and alkaline phosphatase (ALP) activity, microbeads were dissolved overnight in 10 m*M* Tris-HCl (Sigma) containing 0.6 mg/mL COL type I (MP Biomedicals), 0.2% IGEPAL (Sigma), and 2 m*M* phenylmethanesulfonylfluoride (Sigma). DNA content was then assessed using a commercially available DNA assay (PicoGreen®, Life Technologies). Alkaline phosphatase activity was quantified by adding 20 μL of the sample lysate to a 100 μL of 0.5*M* 2-amino-2-methyl-1-popanol (Sigma) with 5.0 m*M* *p*-nitrophenol phosphate substrate (Sigma) at a pH of 10.3 and read spectrophotometrically at 405 nm.[22] Total calcium secretion was analyzed using the ocresolphthalein complexone (OCPC) method as described.[35] Briefly, microbead samples were dissolved overnight in 1.0*N* acetic acid and 10 μL of the sample was incubated in 0.05 mg/ mL of OCPC solution in ethanolamine, boric acid, and 8-hydrox-yquinoline buffer (Sigma) for 10 min. Samples were read against a standard curve with known calcium values at 565 nm.

Statistical analysis

All values are represented as mean ± standard deviation. $N = 4$ independent samples were used for the osteogenic differentiation studies. DNA content and calcium secretion data were normalized to day 1 values from within each condition. A one-way analysis of variance test (ANOVA) and a two-way ANOVA with a Tukey's *post hoc* analysis were used to determine significance between conditions and groups. A value of $p < 0.05$ was used to determine statistical significance.

RESULTS

Acellular microbead morphology, size, and size distribution

Figure 2 depicts acellular COL/FIB microbeads directly after fabrication and shows their regular spheroidal morphology (panels A–D). Coomasie staining allowed for visualization of microbeads under light microscopy, and microbeads containing HA were dark due to the attenuation of light passing through the microbeads. HA remained well-dispersed and homogeneous throughout the microbeads. Confocal reflectance imaging allowed for the visualization of the microbead architecture (panels E, F). COL/FIB microbeads exhibited a fibrillar structure whereas the COL/FIB/HA microbeads was observed to have homogenous distribution of HA throughout and within its fibrillar structure. The addition of HA did not significantly affect the average size of the microbead populations, and both had an average

diameter of approximately 130 ± 25 μm, with a relatively narrow size distribution (panels G, H).

Cell viability

Cell viability of MSC or ASC in COL/FIB or COL/FIB/HA beads was assessed at days 1 and 7, and vital staining of microbeads is shown in Figure 3. Viability remained high (>90%) at both time points in all conditions as seen by the abundant green staining and low red staining. By day 7, the morphology of the embedded cells began to change as they spread throughout both the matrix and mineral phases of the microbeads.

Confocal reflectance imaging of cell-seeded microbeads

Characterization of matrix architecture was performed using confocal reflectance microscopy, as shown in the representative image in Figure 4. Changes in matrix architecture in cell-seeded microbeads were tracked over a 7-day culture period. At day 1, individual fibers were visible within the COL/FIB microbeads. However, by day 7, both COL/FIB and COL/FIB/HA microbeads became denser and the fibrillar structure of the matrix was less evident. The mineral phase could be discerned in HA-containing microbeads, but did not change over the 7-day culture period.

Osteogenic differentiation

Figure 5 shows DNA, ALP, and calcium secretion data for both MSC and ASC in COL/FIB and COL/FIB/HA microbeads after 14 days in either growth or osteogenic media. In growth medium, there were no significant differences in DNA content at day 7; however, the MSC COL/FIB/HA group exhibited significantly higher DNA content compared to the other conditions at day 14. In osteogenic media, the ASC COL/FIB group showed higher DNA content relative to the other conditions at day 7; however, there were no significant differences at day 14.

ALP activity in microbeads was significantly higher at day 3 in the MSC COL/FIB/HA formulation compared to the MSC COL/FIB microbeads. The MSC COL/FIB/HA microbeads showed significantly higher ALP activity when cultured in osteogenic media, as compared to growth media. Both ASC COL/FIB and MSC COL/FIB/HA had statistically greater ALP activity than the MSC COL/FIB microbeads when cultured in osteogenic media.

Calcium deposition markedly increased at day 14 in both the MSC COL/FIB and ASC COL/FIB microbeads in osteogenic media, relative to microbeads cultured in growth media. However, there were no significant differences in calcium deposition between any of the conditions in osteogenic media at day 14.

A full list of the statistical results generated from two-way ANOVA analyses is provided in the tables in Figure 6.

DISCUSSION

This study has demonstrated that a simple water-in-oil emulsion process can be used to create modular microenvironments consisting of native extracellular matrix proteins supplemented with a ceramic phase. The addition of HA into the microbeads increased the yield that was harvested, but did not alter the size or size distribution of the microbeads. COL/FIB and COL/FIB/HA microbeads were spheroidal and approximately 130 μm ± 25 μm in diameter. In this range of microbead sizes, a defined number of cells can be encapsulated within each bead, but cells can also spread and interact with the microbead matrix. Further, this size allows sufficient mass transfer through the microbead matrix to the embedded cells, since the maximum diffusion path for nutrients through tissues has been suggested to be only 150–200 μm.[36] Although not explored in this study, the microbead size and distribution can be controlled by modulating the impeller speed, oil viscosity, and other fabrication process parameters.[31,32]

Analysis of cell viability showed that both MSC and ASC survived the embedding process and remained viable over at least a week in culture. Furthermore, after 7 days both MSC and ASC exhibited a spread morphology indicating that they associated with the COL and FIB extracellular matrix components. Inclusion of HA in the microbeads did not alter either cell type's viability or morphology. In addition, confocal reflectance microscopy allowed the microarchitecture of microbeads to be visualized. The fibrillar structure of the microbeads became denser over time, suggesting that the microbeads were compacted by the embedded cells, a phenomenon that is commonly observed when cells are seeded within natural biomaterials.[37] Taken together, these findings suggest that the microbead environment is conducive to maintenance of living cells and allows them to retain their active functions.

Comparison of MSC and ASC osteogenic differentiation in COL/FIB and COL/FIB/HA microbeads suggested that theses cell types are mostly similar in their responses. Two-way ANOVA found no significant differences between ASC and MSC in their DNA content, ALP activity, or calcium secretion over two weeks of culture in either growth or osteogenic media. Moreover, we did not observe any significant differences between the COL/FIB and COL/FIB/HA matrices in any of the assays, indicating that the addition of HA did not cause any detrimental effects to stem cell differentiation throughout the culture period. ALP activity, an early osteogenic marker, was somewhat elevated in the MSC COL/FIB/HA group, suggesting potential osteoinductive effects of the COL/FIB microbeads. Calcium secretion, a late osteogenic marker, increased in both MSC and ASC in COL/ FIB microbeads in osteogenic media compared to growth media. There were no differences in calcium secretion of either MSC or ASC in COL/FIB/HA microbeads in the two media types, presumably because these matrices already contained a large amount of exogenous mineral.[38]

The modular microbead technology we have demonstrated is aimed at developing new minimally invasive techniques for bone repair. Fabrication of microbeads can be easily scaled up to create larger populations of microbeads in a controlled batch process. Cell-seeded microbeads can be pre-differentiated toward the osteogenic phenotype, collected, concentrated into a paste, and then injected into a defect site in a minimally invasive

manner. The advantages of such a cell-based therapy are particularly important in treating recalcitrant bone wounds and non-unions, where the delivery of appropriately functional cells may be a key to achieving regeneration.

CONCLUSIONS

Stem cell-seeded COL/FIB and COL/FIB/HA microbeads are another tool for modular tissue engineering, and these formulations have particular promise in orthopedic applications. The embedded MSC and ASC remained viable, exhibited remodeling behavior, and mineralized the matrix in response to osteogenic cues. This study found only modest differences in the osteogenic response of MSC and ASC, indicating that either cell type may be a suitable source for bone tissue engineering.

Acknowledgments

Contract grant sponsor: National Science Foundation Graduate Research Fellowship Grant; contract grant number: DGE 1256260

Contract grant sponsor: AO Foundation Large Bone Defect Healing Consortium

References

1. Langer R, Vacanti JP. Tissue engineering. Science. 1993; 260:920–926. [PubMed: 8493529]
2. Szpalski C, Barbaro M, Sagebin F, Warren SM. Bone tissue engineering: Current strategies and techniques—Part II: Cell types. Tissue Eng Part B Rev. 2012; 18:258–269. [PubMed: 22224439]
3. Domev H, Amit M, Laevsky I, Dar A, Itskovitz-Eldor J. Efficient engineering of vascularized ectopic bone from human embryonic stem cell-derived mesenchymal stem cells. Tissue Eng Part A. 2012; 18:2290–2302. [PubMed: 22731654]
4. Thein-Han W, Xu HH. Collagen-calcium phosphate cement scaffolds seeded with umbilical cord stem cells for bone tissue engineering. Tissue Eng Part A. 2011; 17:2943–2954. [PubMed: 21851269]
5. Atari M, Caballé-Serrano J, Gil-Recio C, Giner-Delgado C, Martínez-Sarrà E, García-Fernández DA, Barajas M, Hernández-Alfaro F, Ferrés-Padró E, Giner-Tarrida L. The enhancement of osteogenesis through the use of dental pulp pluripotent stem cells in 3D. Bone. 2012; 50:930–941. [PubMed: 22270057]
6. Lee K, Chan CK, Patil N, Goodman SB. Cell therapy for bone regeneration—Bench to bedside. J Biomed Mater Res B Appl Bio-mater. 2009; 89:252–263.
7. Wang J, Yang Q, Mao C, Zhang S. Osteogenic differentiation of bone marrow mesenchymal stem cells on the collagen/silk fibroin bi-template-induced biomimetic bone substitutes. J Biomed Mater Res. 2012; 100:2929–2938.
8. Hattori H, Masuoka K, Sato M, Ishihara M, Asazuma T, Takase B, Kikuchi M, Nemoto K, Ishihara M. Bone formation using human adipose tissue-derived stromal cells and a biodegradable scaffold. J Biomed Mater Res B Appl Biomater. 2006; 76:230–239. [PubMed: 16047328]
9. English K, Mahon BP. Allogeneic mesenchymal stem cells: Agents of immune modulation. J Cell Biochem. 2011; 8:1963–1968. [PubMed: 21445861]
10. Gir P, Oni G, Brown SA, Mojallal A, Rohrich RJ. Human adipose stem cells: Current clinical applications. Plast Reconstr Surg. 2012; 129:1277–1290. [PubMed: 22634645]
11. Strioga M, Viswanathan S, Darinskas A, Slaby O, Michalek J. Same or not the same? Comparison of adipose tissue-derived versus bone marrow-derived mesenchymal stem and stromal cells. Stem Cells Dev. 2012; 21:2724–2752. [PubMed: 22468918]
12. Shafiee A, Seyedjafari E, Soleimani M, Ahmadbeigi N, Dinarvand P, Ghaemi N. A comparison between osteogenic differentiation of human unrestricted somatic stem cells and mesenchymal

stem cells from bone marrow and adipose tissue. Biotechnol Lett. 2011; 33:1257–1264. [PubMed: 21287233]

13. Miyazaki M, Zuk PA, Zou J, Yoon SH, Wei F, Morishita Y, Sintuu C, Wang JC. Comparison of human mesenchymal stem cells derived from adipose tissue and bone marrow for ex vivo gene therapy in rat spinal fusion model. Spine. 2008; 33:863–869. [PubMed: 18404105]
14. Noël D, Caton D, Roche S, Bony C, Lehmann S, Casteilla L, Jorgensen C, Cousin B. Cell specific differences between human adipose-derived and mesenchymal-stromal cells despite similar differentiation potentials. Exp Cell Res. 2008; 314:1575–1584. [PubMed: 18325494]
15. De Ugarte DA, Morizono K, Elbarbary A, Alfonso Z, Zuk PA, Zhu M, Dragoo JL, Ashjian P, Thomas B, Benhaim P, Chen I, Fraser J, Hedrick MH. Comparison of multi-lineage cells from human adipose tissue and bone marrow. Cells Tissues Organs. 2003; 174:101–109. [PubMed: 12835573]
16. Gao TJ, Lindholm TS, Kommonen B, Ragini P, Paronzini A, Lindholm TC. Enhanced healing of segmental tibial defects in sheep by a composite bone substitute composed of tricalcium phosphate cylinder, bone morphogenetic protein, and type IV collagen. J Biomed Mater Res. 1996; 32:505–512. [PubMed: 8953139]
17. Jégoux F, Goyenvalle E, Cognet R, Malard O, Moreau F, Daculsi G, Aguado E. Reconstruction of irradiated bone segmental defects with a biomaterial associating MBCP+®, microstructured collagen membrane and total bone marrow grafting: An experimental study in rabbits. J Biomed Mater Res Part A. 2009; 91:1160–1169.
18. Guda T, Walker JA, Singleton BM, Hernandez JW, Son JS, Kim SG, Oh DS, Appleford M, Ong JL, Wenke JC. Guided bone regeneration in long bone defects with a structural hydroxyapatite graft and collagen membrane. Tissue Eng Part A. 2013 Epub Ahead of Print.
19. Le Nihouannen D, Saffarzadeh A, Aguado E, Goyenvalle E, Gauthier O, Moreau F, Pilet P, Spaethe R, Daculsi G, Layrolle P. Osteogenic properties of calcium phosphate ceramics and fibrin glue based composites. J Mater Sci Mater Med. 2007; 18:225–235. [PubMed: 17323153]
20. Davis HE, Miller SL, Case EM, Leach JK. Supplementation of fibrin gels with sodium chloride enhances physical properties and ensuing osteogenic response. Acta Biomater. 2011; 7:691–699. [PubMed: 20837168]
21. Muzzarelli RA, Biagini G, Bellardini M, Simonelli L, Castaldini C, Fratto G. Osteoconduction exerted by methylpyrolidinone chitosan in dental surgery. Biomaterials. 1993; 14:39–43. [PubMed: 8425023]
22. Wang L, Stegemann JP. Glyoxal crosslinking of cell-seeded chitosan/collagen hydrogels for bone regeneration. Acta Biomater. 2011; 7:2410–2417. [PubMed: 21345389]
23. Koo KT, Polimeni G, Qahash M, Kim CK, Wikesjö UM. Periodontal repair in dogs: guided tissue regeneration enhances bone formation in sites implanted with a coral-derived calcium carbonate biomaterial. J Clin Periodontol. 2005; 32:104–110. [PubMed: 15642067]
24. Jones JR. Review of bioactive glass- from Hench to hybrids. Acta Biomater. 2013; 9:4457–4486. [PubMed: 22922331]
25. Rao RR, He J, Leach JK. Biomineralized composite substrates increase gene expression with nonviral delivery. J Biomed Mater Res A. 2010; 94:344–354. [PubMed: 20186740]
26. Gleeson JP, Plunkett NA, O'Brien FJ. Addition of hydroxyapatite improves stiffness, interconnectivity and osteogenic potential of a highly porous collagen-based scaffold for bone tissue regeneration. Eur Cell Mater. 2010; 20:218–230. [PubMed: 20922667]
27. Yoshikawa H, Myoui A. Bone tissue engineering with porous hydroxyapatite ceramics. J Artif Organs. 2005; 8:131–136. [PubMed: 16235028]
28. Nichol JW, Khademhosseini A. Modular tissue engineering: Engineering Biological tissues from the bottom up. Soft Matter. 2009; 5:1312–1319. [PubMed: 20179781]
29. Chen M, Wang X, Ye Z, Zhang Y, Zhou Y, Tan WS. A modular approach to the engineering of a centimeter-sized bone tissue construct with human amniotic mesenchymal stem cells-laden microcarriers. Biomaterials. 2011; 32:7532–7542. [PubMed: 21774980]
30. Tang M, Chen W, Weir MD, Thein-Han W, Xu HH. Human embryonic stem cell encapsulation in alginate microbeads in macroporous calcium phosphate cement for bone tissue engineering. Acta Biomater. 2012; 8:3436–3445. [PubMed: 22633970]

31. Chen Z, Wang L, Stegemann JP. Phase-separated chitosan-fibrin microbeads for cell delivery. J Microencapsul. 2011; 28:344–352. [PubMed: 21736519]
32. Batorsky A, Liao J, Lund AW, Plopper GE, Stegemann JP. Encapsulation of adult human mesenchymal stem cells within collagen-agarose microenvironments. Biotechnol Bioeng. 2005; 92:492–500. [PubMed: 16080186]
33. Wang L, Rao RR, Stegemann JP. Matrix-enhanced stem cells embedded in chitosan-collagen microbeads. Cells, Tissues Organs. 2013 in press.
34. Lund AW, Bush JA, Plopper GE, Stegemann JP. Osteogenic differentiation of mesenchymal stem cells in defined protein beads. J Biomed Mater Res B Appl Biomater. 2008; 87:213–221. [PubMed: 18431753]
35. Gudur M, Rao RR, Hsiao YS, Peterson AW, Deng CX, Stegemann JP. Noninvasive, quantitative, spatiotemporal characterization of mineralization in three-dimensional collagen hydrogels using high-resolution spectral ultrasound imaging. Tissue Eng Part C. Forthcoming.
36. Novosel EC, Kleinhans C, Kluger PJ. Vascularization is the key challenge in tissue engineering. Adv Drug Deliv Rev. 2011; 63:300–311. [PubMed: 21396416]
37. Fernandez P, Bausch AR. The compaction of gels by cells: A case of collective mechanical activity. Integr Biol (Camb). 2009; 1:252–259. [PubMed: 20023736]
38. Davis HE, Rao RR, He J, Leach JK. Biomimetic scaffolds fabricated from apatite-coated polymer microspheres. J Biomed Mater Res A. 2009; 90:1021–1031. [PubMed: 18655148]

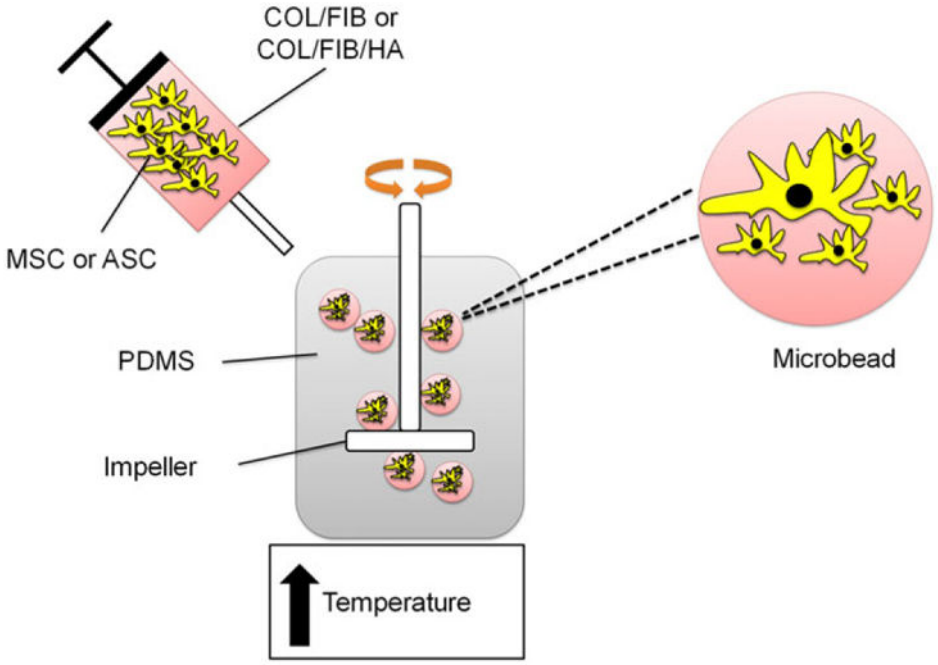

FIGURE 1.

Schematic of microbead fabrication process. COL/FIB and COL/FIB/HA microbeads were formed through a water-in-oil emulsification process which resulted in spherical three-dimensional cell-seeded hydrogel microenvironments. [Color figure can be viewed in the online issue, which is available at wileyonlinelibrary.com.]

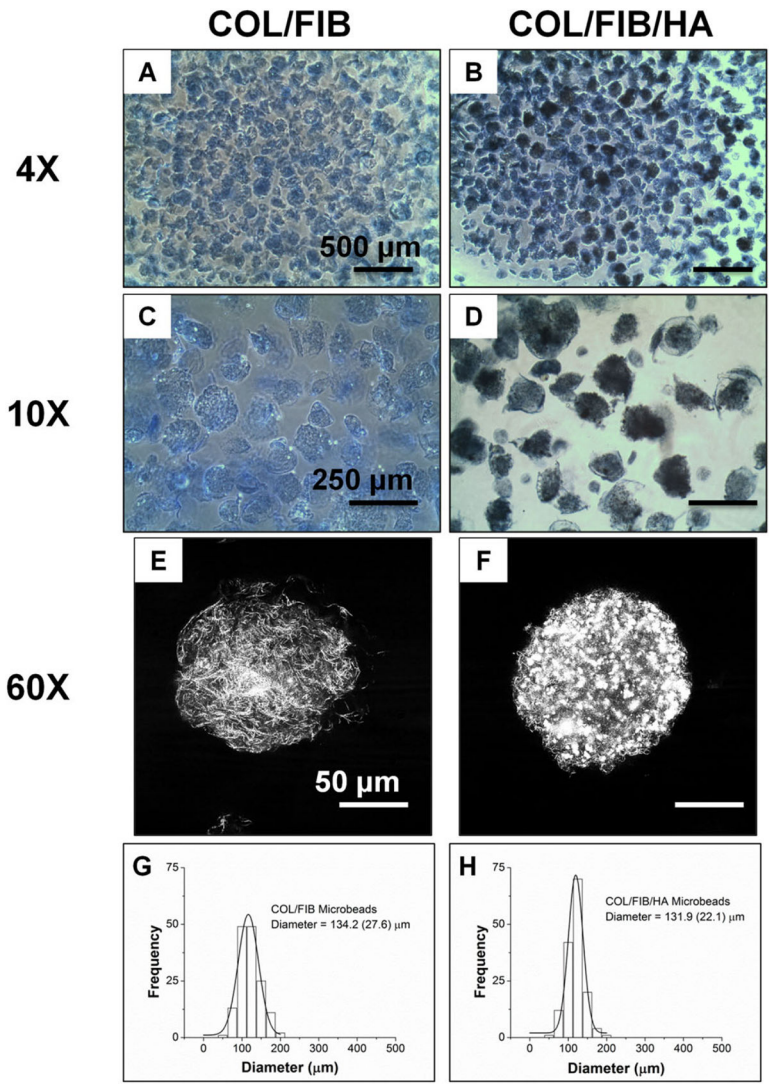

FIGURE 2.

Morphology and size distribution of acellular microbeads. Coomasie staining allowed for visualization of microbeads under light microscopy (4×, 10×). Images of the microarchitecture of microbeads obtained through confocal reflectance (60×). The addition of HA did not alter the size or the size distribution of microbeads. [Color figure can be viewed in the online issue, which is available at wileyonlinelibrary.com.]

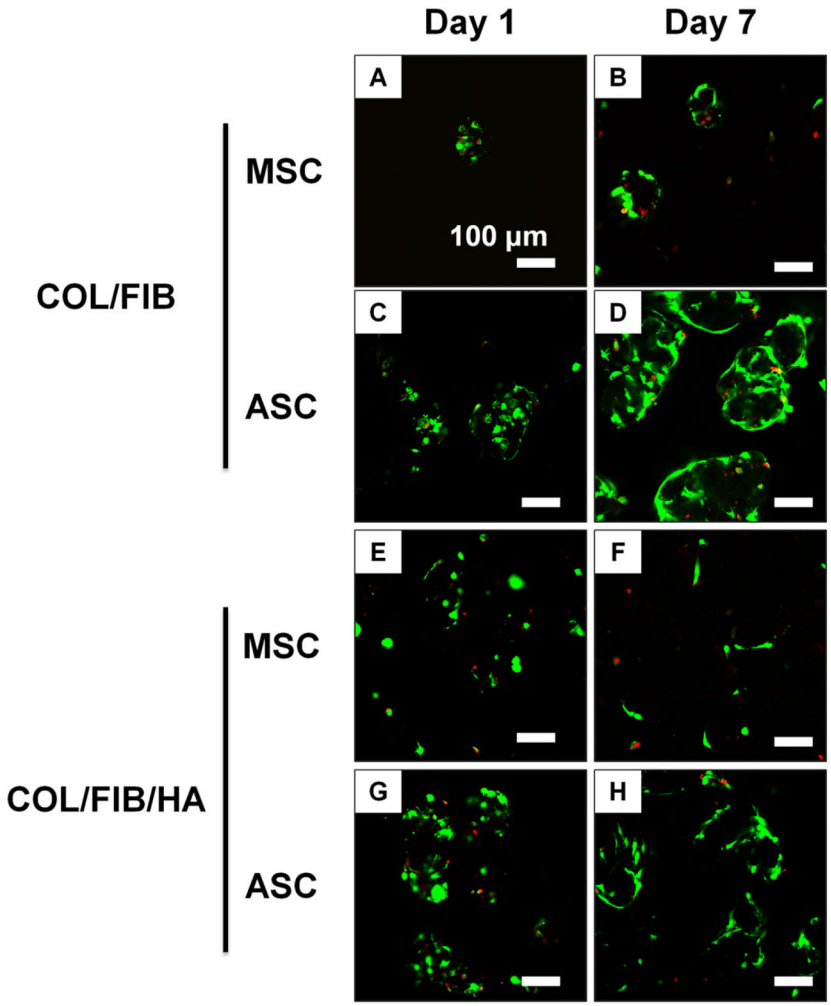

FIGURE 3.

Cell viability of MSC or ASC in COL/FIB or COL/FIB/HA microbeads at days 1 and 7. Scale bar = 100 μm. [Color figure can be viewed in the online issue, which is available at wileyonlinelibrary.com.]

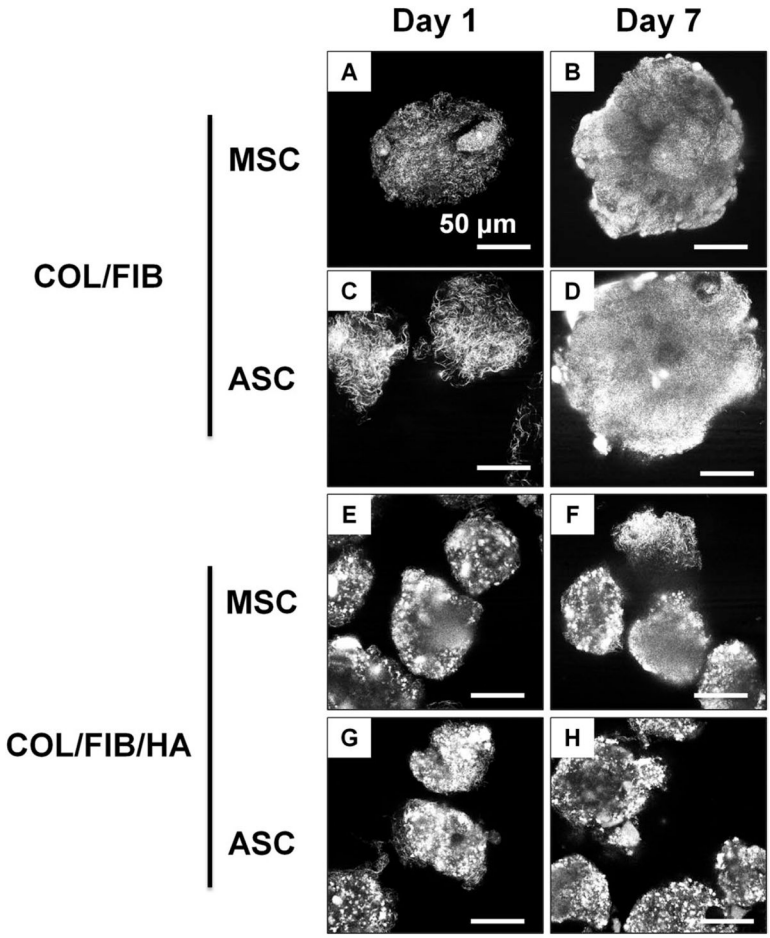

FIGURE 4.

Confocal reflectance imaging of MSC or ASC in COL/FIB or COL/FIB/HA microbeads at days 1 and 7. Scale bar = 50 μm.

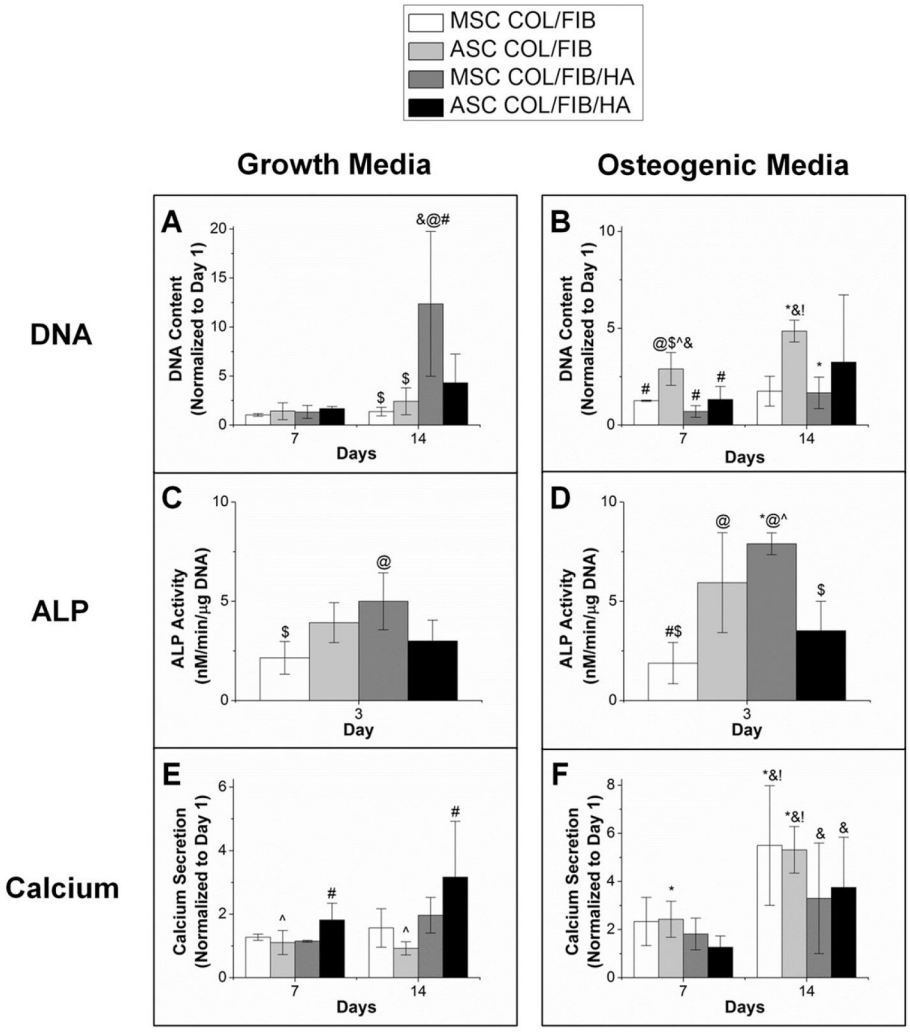

FIGURE 5.

Osteogenic differentiation. (*) denotes statistical significance against growth condition. (@) denotes statistical significance against MSC COL/FIB. (#) denotes statistical significance against ASC COL/FIB. ($) denotes statistical significance against MSC COL/FIB/HA. (^) denotes statistical significance against ASC COL/FIB/HA. (&) denotes statistical significance against day 1. (!) denotes statistical significance against day 7.

DNA	Day 7		Day 14	
	Significant	p value	Significant	p value
MSC vs. ASC	X	0.001		0.671
Growth vs. Osteo		0.460		0.128
COL/FIB vs. COL/FIB/HA		0.110		0.057

ALP	Day 3	
	Significant	p value
MSC vs. ASC		0.656
Growth vs. Osteo		0.057
COL/FIB vs. COL/FIB/HA		0.087

Calcium	Day 7		Day 14	
	Significant	p value	Significant	p value
MSC vs. ASC		0.962		0.710
Growth vs. Osteo	X	0.014	X	0.0003
COL/FIB vs. COL/FIB/HA		0.247		0.663

FIGURE 6.
Two-way Analysis of Variance (ANOVA) results.